

Phase Behavior of Blends of Polymers and Smectic-A Liquid Crystals

Farida Benmouna,[†] Xavier Coqueret,[‡] Ulrich Maschke,^{*,‡} and Mustapha Benmouna[†]*Institut de Chimie, Université Aboubakr Belkaid, BP119, Tlemcen 13000, Algeria, and Laboratoire de Chimie Macromoléculaire, Université des Sciences et Technologies de Lille, CNRS URA 351, 59655 Villeneuve d'Ascq Cedex, France**Received March 16, 1998; Revised Manuscript Received May 13, 1998*

ABSTRACT: The phase behavior of blends of polymers and smectic-A liquid crystals (LCs) is investigated using Flory–Huggins and Maier–Saupe–McMillan theories. Various examples are considered to depict the effects of the architecture and the size of the polymer together with the nature of anisotropic ordering forces on the phase diagram. The strength of these forces is characterized by a parameter α which is directly related to the temperature of the smectic–nematic transition. Three cases are considered depending on the value of α , and the corresponding phase diagrams are constructed. Substantial differences are observed in these diagrams, and the reasons for these differences are discussed. A comparative study is performed between mixtures of polymers and LCs, where the polymer is made of linear and crosslinked chains. The LC consists either of molecules with nematic ordering only or of molecules presenting both nematic and smectic-A ordering. Blends where polymer matrices are cross-linked networks are also examined. Remarkable properties are found in the nature of the phase diagrams for such mixtures. In general, it is observed that the ordering forces favor unmixing with a stronger effect for the higher smectic-A ordering. Spinodal curves are also reported for these mixtures. The effects of fluctuations near the transition temperatures are briefly discussed.

1. Introduction

Mixtures of polymers and liquid crystals (LCs) are interesting systems from various points of view. In particular, PDLCs (polymer dispersed liquid crystals) have considerable potential for various electrooptical applications such as flexible displays and switchable windows.^{1–4} In their most common form, PDLC films consist of low molecular weight LC microdroplets dispersed in a solid polymer matrix.

PDLC systems are prepared in our laboratory by exposure of the reactive solutions to electron beam radiation.^{5–8} The initial solutions are made of mixtures of monomers, oligomers, and nematic LCs. The cross-linking and polymerization of the polymer precursors by the radiation process leads to phase separation between the polymer matrix and the LCs. This procedure is known as polymerization induced phase separation (PIPS) and is not limited to the electron beam radiation. Therefore, it is important to realize that the obtained polymer matrix is a cross-linked network which is characterized by a different phase behavior as compared to a polymer matrix made of free chains.

Theoretically, PDLC systems can be considered as multicomponent mixtures characterized by a rich phase behavior.^{9–11} In a recent paper,¹² we reported some phase diagrams of mixtures of polymers and nematic LCs. Two types of interactions were considered: The first one is an isotropic interaction introduced via the Flory–Huggins¹³ lattice model, and the second is an anisotropic interaction described within the Maier–Saupe^{14,15} theory for nematic ordering. A systematic study of the phase properties of mixtures including LCs and linear polymer chains was performed. In particu-

lar, it was observed that increasing the polymer length results in widening of the miscibility gap.

Moreover, the area of the single nematic phase observed near $\varphi_1 = 1$ reduces dramatically. Likewise, increasing the size of LC molecules leads to similar observations. Another case where the Flory–Huggins interaction parameter χ was increased, while the temperature was maintained constant was also considered. It was found that the miscibility gap becomes wider while the region of single nematic phase was not modified. Decreasing the temperature below T_{NI} leads to wider regions of single nematic phases and to the appearance of two nematic–isotropic coexisting phases. The phase diagram of blends with cross-linked chains was also studied. Remarkable differences with the case of mixtures with linear polymers were observed.

In the present paper, an attempt is made to extend these investigations to the case where the LC has not only a nematic ordering but also a smectic-A ordering as well. Two order parameters are needed to describe the phase behavior of these mixtures. The anisotropic forces here give rise to at least three different types of transitions, which are nematic–isotropic (NI), smectic–nematic (SN), and smectic–isotropic (SI) transitions. Phase diagrams for mixtures containing smectic-A LCs and either linear or cross-linked polymers are established.

A theoretical study dealing with hypothetical polymer/LC mixtures is performed, where parameter values are chosen comparable to those reported in the literature. Considering hypothetical blends can help in identifying new trends in the phase properties possibly emerging in new applications or in upgrading performances of known applications. The present investigation allows one to see in what direction and to what extend the phase diagrams are distorted by changing one or several parameters of the mixture, i.e., the interaction parameter χ , the temperature T , etc.

* To whom correspondence should be addressed. E-mail: maschke@univ-lille1.fr.

[†] Université Aboubakr Belkaid.

[‡] Université des Sciences et Technologies de Lille.

2. Theoretical Formalism

Recently, Shen and Kyu¹⁶ presented a theoretical formalism describing the phase behavior of smectic-A LCs and linear polymers. This formalism is based upon the Flory–Huggins¹³ lattice model for isotropic mixing and the Maier–Saupe–McMillan^{14,15,17} theory for anisotropic ordering.

This description is used to perform a systematic study of the phase behavior of mixtures with smectic-A ordering and several values of the parameter α and the temperature of smectic–nematic (SN) transition T_{SN} . This study is extended to the case of cross-linked polymers, for which the phase behavior is remarkably different compared to the case of linear polymers.

The starting point is to write the expression of the free energy density f (per site) which is a sum of two terms. The first term represents the free energy for isotropic mixing while the second is the free energy for anisotropic ordering. Denoting with F the free energy for the whole lattice and with f the free energy per site (free energy density), and assuming that there are n_0 sites in the lattice, one writes

$$f = f^{(i)} + f^{(a)} = \frac{F}{n_0} = \frac{F^{(i)} + F^{(a)}}{n_0} \quad (1)$$

The superscripts (i) and (a) stand for isotropic and anisotropic, respectively. As pointed out earlier, both linear and cross-linked polymer matrices are considered. The main difference between these two systems resides in the form of the isotropic free energy. It is assumed that the polymer component has no mesogenic parts. Discussions of isotropic free energies are given in the next section. The anisotropic contribution is assumed to be independent of the polymer architecture and will be examined in a later section.

2.1. Isotropic Free Energy for Blends of LCs with Linear Polymers. The isotropic free energy of blends of LCs and linear polymers is represented by the Flory–Huggins lattice model¹³

$$\frac{f^{(i)}}{k_B T} = \frac{F^{(i)}}{n_0 k_B T} = \frac{\varphi_1}{N_1} \ln \varphi_1 + \frac{\varphi_2}{N_2} \ln \varphi_2 + \chi \varphi_1 \varphi_2 \quad (2)$$

For an incompressible mixture, all the n_0 sites are occupied and one has

$$n_0 = n_1 N_1 + n_2 N_2 \quad (3)$$

$F^{(i)}$ is the isotropic free energy for the entire lattice, N_1 and N_2 are the numbers of repeat units (degrees of polymerization), n_1 and n_2 are the numbers of molecules, and φ_1 and φ_2 are the volume fractions of components 1 (LC) and 2 (polymer), respectively. All units are assumed to have the same volume, and, therefore, φ_1 and φ_2 represent also the number fractions

$$\varphi_1 = \frac{n_1 N_1}{n_0} = 1 - \varphi_2 \quad (4)$$

The parameter χ in eq 2 is the Flory–Huggins interaction parameter for the polymer/LC blend. It will be assumed to satisfy the following relationship with temperature T

$$\chi = A + \frac{B}{T} \quad (5)$$

where A and B are constants independent of temperature and composition. They depend only on the nature of molecules in the mixture. If the polymer is a cross-linked network, one should account for the presence of cross-links in the free energy as shown in the next section.

2.2. Isotropic Free Energy for a Blend of a LC and a Cross-Linked Polymer. When the polymer present in the polymer/LC mixture is a cross-linked network, its elasticity is much more important and modifies remarkably the phase behavior. The Flory–Huggins free energy is no longer valid, and one has to rely on another model for the isotropic free energy. The following form is adopted^{18–20}

$$\frac{f^{(i)}}{k_B T} = \frac{F^{(i)}}{n_0 k_B T} = \frac{3\alpha}{2N_c} [\varphi_0^{2/3} \varphi_2^{1/2} - \varphi_2] + \frac{\beta \varphi_2}{N_c} \ln \left(\frac{\varphi_2}{\varphi_0} \right) + \frac{\phi_1 \ln \varphi_1}{N_1} + \chi \varphi_1 \varphi_2 \quad (6)$$

N_c represents the number of monomer units between two consecutive cross-links, and the constants α and β are model dependent. Usually, $\alpha = 1$ and β can take different values, depending upon the model under consideration. James and Guth²¹ proposed to let $\beta = 0$, whereas Hermans²² and Kuhn²³ suggested that $\beta = 1$ and Flory²⁴ proposed that $\beta = 2/(\text{functionality of the monomer at the cross-links})$. The network can be considered as a simple molecule of N_l monomers. In this case, n_0 becomes

$$n_0 = N_l + n_1 N_1 \quad (7)$$

φ_0 represents the polymer volume fraction at the formation of the network, also known as the reference state volume fraction.

The isotropic free energy is the main source of difference between the thermodynamic properties of mixtures with either linear or cross-linked polymers. The impact of such differences on the phase properties of PDLC materials is remarkable. The total free energy required to investigate these properties contains two contributions. One of them is the isotropic free energy of mixing, while the other arises from the nematic and the smectic ordering forces. The latter contribution is common to linear and cross-linked polymers and is the subject of the following section.

2.3. The Maier–Saupe–McMillan Anisotropic Free Energy. The anisotropic forces induce either nematic or smectic ordering, depending upon the temperature range under consideration. This is derived from a model of the free energy which combines the Maier–Saupe and the McMillan^{14,15,17} theories. The former describes the case of nematic LCs, while the latter is a generalization to the smectic-A LCs

$$\frac{f^{(a)}}{k_B T} = \frac{F^{(a)}}{n_0 k_B T} = \frac{\varphi_1}{N_1} \left\{ \int \int g(z, \mu) \ln [4\pi g(z, \mu)] d\mu dz - \frac{1}{2} \nu \varphi_1 (S^2 + \alpha \sigma^2) \right\} \quad (8)$$

where the integration over μ is performed in the range $[0, 1]$, whereas the integration over z should be done in the range $[0, d]$ and normalized with respect to d , the interlayer spacing along the z axis in the smectic-A ordering. The double integral represents the decrease

of entropy resulting from alignments of LC molecules, and the second term on the right-hand side describes the combined effects of nematic and smectic interactions. The following change of variables was made implicitly in eq 8, $\mu = \cos \theta$, where θ is the angle between the director of LC molecules and the reference axis z . The function $g(z, \mu)$ represents the distribution of director orientations

$$g(z, \mu) = \frac{\exp[-(u_n + u_s)/k_B T]}{4\pi Z} \quad (9)$$

where u_n and u_s are potential fields for nematic and smectic orderings, respectively. Within the Maier–Saupe–McMillan theory, the latter quantities are expressed in terms of the mean field parameters m_n and m_s characterizing the strengths of interactions

$$\frac{u_n}{k_B T} = -\frac{m_n}{2}(3\mu^2 - 1) \quad (10)$$

$$\frac{u_s}{k_B T} = -\frac{m_s}{2}(3\mu^2 - 1) \cos\left(\frac{2\pi z}{d}\right) \quad (11)$$

The capital letter Z represents the partition function

$$Z = \int \int d\mu dz \exp\left[\frac{m_n}{2}(3\mu^2 - 1)\right] \exp\left[\frac{m_s}{2}(3\mu^2 - 1) \cos\left(2\pi \frac{z}{d}\right)\right] \quad (12)$$

In this description, two order parameters are needed. The first one is the nematic order parameter S

$$S = \langle \frac{1}{2}(3 \cos^2 \theta - 1) \rangle \quad (13)$$

and the second order parameter σ is related to the smectic-A ordering along the z -direction

$$\sigma = \frac{1}{2} \left\langle \cos\left(\frac{2\pi z}{d}\right) (3 \cos^2 \theta - 1) \right\rangle \quad (14)$$

The symbol $\langle \dots \rangle$ represents the average with respect to the distribution function $g(z, \mu)$; ν , the Maier–Saupe quadrupole interaction parameter for nematic ordering; and α , the McMillan interaction strength of the smectic-A ordering. The parameter ν is inversely proportional to the temperature:

$$\nu = 4.54 \frac{T_{NI}}{T}, \quad T_{NI} = 333 \text{ K} \quad (15)$$

T_{NI} represents the nematic–isotropic transition temperature of the pure nematic LC. The proportionality constant changes slightly with the nature of the LC. Here, we select values available in the literature and attributed to the nematic LC mixture known as E7.^{14,15,25} Therefore, the transition temperature T_{NI} will be 60 °C and the proportionality constant 4.54 as indicated in eq 15.

The parameter α depends on the interlayer distance d via the relationship

$$\alpha = \exp[-(\pi l/d)^2] \quad (16)$$

α is zero when d is small compared to the molecular size l and 2 when d is large.¹⁷ The interlayer spacing d

is fixed by an interplay between anisotropic and steric forces. The former are larger for higher values of α and d . If d exceeds the molecular size, then the LC molecules are tightly packed in the plane, but this configuration is energetically unfavorable. A more likely configuration corresponds to the situation where d is of the order of the molecular size l . The anisotropic forces are due to the rigid parts, while steric forces are due to the high excluded volume, generated by the long flexible tails of the LC molecules requiring higher interplanar distances.

Combining eqs 9 and 14, one can express the order parameters S and σ in terms of the partition function Z only

$$S = \frac{1}{Z} \frac{\partial Z}{\partial m_n} = \frac{\partial}{\partial m_n} \ln Z \quad (17)$$

$$\sigma = \frac{1}{Z} \frac{\partial Z}{\partial m_s} = \frac{\partial}{\partial m_s} \ln Z \quad (18)$$

The entropic term in the anisotropic free energy can be expressed in terms of Z , S , and σ as follows:

$$\int \int d\mu dz g(z, \mu) \ln[4\pi g(z, \mu)] = \ln Z - m_n S - m_s \sigma \quad (19)$$

Minimization of the free energy with respect to the order parameters yields a relationship between S , σ , and the strengths of potential fields m_n and m_s . Therefore, letting

$$\partial f^{(a)}/\partial S = 0 \quad \partial f^{(a)}/\partial \sigma = 0 \quad (20)$$

yields the important relationships between m_n and m_s and the relevant parameters describing directly the thermodynamic state of the mixture

$$m_n = \nu S \varphi_1 \quad m_s = \alpha \nu \sigma \varphi_1 \quad (21)$$

Combining eqs 8–14 and eqs 20 and 21 lead to the final result for the anisotropic free energy of smectic-A LCs. This result can be expressed in terms of the partition function and the order parameters

$$\frac{f^{(a)}}{k_B T} = \frac{\varphi_1}{N_1} \left[-\ln Z + \frac{1}{2} \nu \varphi_1 (S^2 + \alpha \sigma^2) \right] \quad (22)$$

In the absence of smectic ordering, α is zero and one recovers the results of nematic LC (eq 2 in ref 12).

3. Results and Discussions

3.1. Order Parameters S and σ . To establish the variation of the order parameters S and σ with composition and temperature, one needs to perform a self-consistent numerical resolution of eqs 12, 17, 18, and 21. At this stage, it is convenient to introduce the zeroth order modified Bessel function²⁶

$$I_0(x) = \frac{1}{\pi} \int_0^\pi \exp(x \cos \beta) d\beta \quad (23)$$

The partition function can be written using $I_0(x)$ simply as follows:

$$Z = \int_0^1 d\mu \exp\left[\frac{m_n}{2}(3\mu^2 - 1)\right] I_0\left(\frac{m_s}{2}(3\mu^2 - 1)\right) \quad (24)$$

In the present investigation, we cover a range of temperatures and compositions in such a way that the argument of the Bessel function $x \equiv m_s(3\mu^2 - 1)/2$ does not exceed 5. In these conditions, the numerical resolution is simplified further if one replaces the modified Bessel function $I_0(x)$ by its approximate forms. The following approximations prove to be useful.²⁶

If the argument x is less than 3.75, the Bessel function $I_0(x)$ can be replaced by

$$I_0(x) = 1 + 3.5156229t^2 + 3.0899424t^4 + 1.2067492t^6 + 0.2659732t^8 + 0.0360768t^{10} + 0.0045813t^{12} + \epsilon \quad (25)$$

$$\text{with } |\epsilon| < 1.6 \times 10^{-7} \text{ and } t \equiv x/3.75$$

If the argument x is higher than 3.75, one could use the following approximation

$$x^{1/2} \exp(-x) I_0(x) \approx 0.39894228 + 0.01328592t^{-1} + 0.00225319t^{-2} - 0.00157565t^{-3} + 0.00916281t^{-4} - 0.02057706t^{-5} + 0.02635537t^{-6} - 0.01647633t^{-7} + 0.00392377t^{-9} + \epsilon \quad (26)$$

$$\text{with } t \equiv x/3.75 \text{ and } |\epsilon| < 1.9 \times 10^{-7}$$

The argument x rarely exceeds 3.75 for the systems under consideration, and the approximate form given by eq 25 is sufficient within a negligible error (less than 10⁻³%). Moreover, the anisotropic forces are nonzero only if the order parameters S and σ exceed some threshold values S_c and σ_c . Above the nematic–isotropic transition temperature T_{NI} and below the volume fraction φ_{NI} , there is no nematic ordering. Likewise, above the smectic–nematic transition temperature T_{SN} and below the volume fraction φ_{SN} , there is no smectic ordering. The couples (T_{NI}, φ_{NI}) and (T_{SN}, φ_{SN}) satisfy the following relationships at each temperature T

$$\varphi_{NI} = \frac{T}{T_{NI}} \quad \varphi_{SN} = \frac{T}{T_{SN}} \quad (27)$$

According to the McMillan¹⁷ theory, T_{SN} increases with the parameter α and reaches T_{NI} at $\alpha = 0.98$. The empirical parameter α seems to determine the nature of the transition, and depending upon its value, one has the sequence of transitions of either smectic–nematic–isotropic or a direct smectic–isotropic transition. If α exceeds the value 0.98, a direct transition from the smectic to the isotropic phase takes place. For α smaller than 0.98, the phase transition process goes through the sequence smectic–nematic–isotropic. To illustrate these results, we have plotted in Figure 1a–c the variations of the order parameters S and σ as functions of φ_1 for several temperatures and (a) $\alpha = 0.851$ ($T_{SN} = 40^\circ\text{C}$), (b) $\alpha = 0.9$ ($T_{SN} = 45^\circ\text{C}$), and (c) $\alpha = 0.98$ ($T_{SN} = T_{NI} = 60^\circ\text{C}$). The thick and dashed curves represent S and σ , respectively. The nematic–isotropic transition temperature is the same for the three systems ($T_{NI} = 60^\circ\text{C}$). The temperature increases from left to right in the three figures, and the range of composition where the order parameters are nonzero reduces as T increases. For a given composition, the order parameters are larger as the temperature decreases. Parts a and b of Figure 1 show qualitatively the same behavior. The order

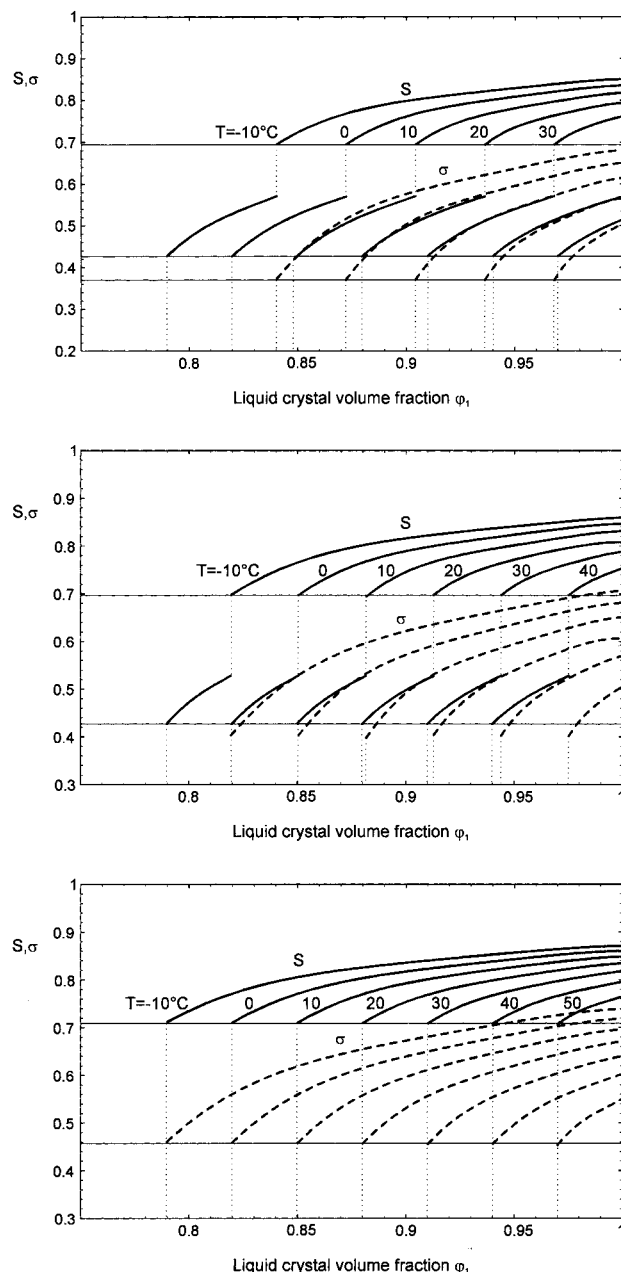


Figure 1. (a, top) Variation of the order parameters S and σ as functions of φ_1 for several temperatures, as indicated on the figure, and $\alpha = 0.851$ ($T_{SN} = 40^\circ\text{C}$). The thick and dashed curves represent S and σ , respectively. The NI transition temperature is $T_{NI} = 60^\circ\text{C}$. (b, middle) Same as a for $\alpha = 0.9$ ($T_{SN} = 45^\circ\text{C}$). (c, bottom) Same as a for $\alpha = 0.98$ and $T_{SN} = T_{NI} = 60^\circ\text{C}$. a and b show that the thick lines contain two branches indicating smectic–nematic and nematic–isotropic transitions. c has a direct smectic–isotropic transition.

parameter S undergoes two discontinuities. For each temperature, the first discontinuity takes place at φ_{NI} while the nematic order first appears. As φ_1 increases, a second discontinuity appears at the volume fraction φ_{SN} where the smectic order appears. The volume fraction at the transitions shifts to higher LC values when the temperature increases. If the temperature is higher than T_{SN} , the order parameter S undergoes only one discontinuity. At the volume fraction of the smectic–nematic transition, both order parameters S and σ undergo discontinuous changes. The order parameter S shows a certain drop at the same composition φ_{SN} , where σ drops also suddenly (discontinuously) to zero.

Figure 1c reproduces similar plots with $T_{NI} = 60\text{ }^{\circ}\text{C} = T_{SN}$ and $\alpha = 0.98$. At a given temperature, both order parameters S and σ fall to zero discontinuously at the same volume fraction $\varphi_{NI} = \varphi_{SN}$. A direct transition from a smectic-A to an isotropic phase takes place without going through a nematic phase. Parts a and b of Figure 1 show also discontinuous drops of S to zero at the nematic–isotropic transition composition φ_{NI} . According to McMillan theory, the smectic–nematic transition is second order if $\alpha < 0.7$ and first order if α is between 0.7 and 0.98.

Once the variations of order parameters with temperature and composition are known, one can proceed to study the phase properties of polymer/LC mixtures in various conditions.

3.2. Free energies and phase diagrams for blends of smectic-A LCs and linear polymers. (a) **Free Energy.** To establish the phase diagram of mixtures of linear polymers and smectic-A LCs, it is useful to examine first the free energy curves as a function of composition and temperature. From the order parameter curves in Figure 1a–c, at certain temperatures, one expects that the curvature of the free energy versus φ_1 undergoes sudden changes at φ_{NI} and φ_{SN} . To see these changes together with the effects of nematic and smectic ordering forces on the free energy, a hypothetical mixture is chosen, characterized by parameter values similar to those considered in our previous investigation dealing with nematic LCs¹²

$$N_1 = 4, \quad N_2 = 10, \quad \chi = -0.34 + \frac{225}{T} \quad (28)$$

Figure 2a represents the variation of the free energy as a function of φ_1 at $T = 39\text{ }^{\circ}\text{C}$ for a mixture characterized by $\alpha = 0.851$ or $T_{SN} = 40\text{ }^{\circ}\text{C}$ and $T_{NI} = 60\text{ }^{\circ}\text{C}$. For a nematic LC, at the present temperature, the free energy curve admits only one double tangent. Looking at Figure 2a, one may think that the free energy curve admits also a double tangent. In fact, a detailed calculation using the standard procedure of chemical potential equalities of the two components in coexisting phases reveals a triple tangent behavior at this temperature. To see this behavior, we present in Figure 2b an enlarged view of Figure 2a in the vicinity of $\varphi_1 = 1$. It is clear that the tangent going through points B and C extends to point A of Figure 2a. To establish the full phase diagram, one needs to repeat similar plots and enlarged views near $\varphi_1 = 1$ in a wide range of temperatures covering a region from below to above T_{NI} . Such plots were made for the three smectic LCs characterized by different values of the smectic–nematic transition temperature. For example, the LC with $\alpha = 0.9$ and $T_{SN} = 48\text{ }^{\circ}\text{C}$ has properties roughly similar to the preceding ones used in Figure 2. This similarity can be observed both from Figure 1b representing the order parameters and from Figure 3a,b, representing the free energy versus composition at $T = 46.3\text{ }^{\circ}\text{C}$. Figure 3a shows features different from those of Figure 2a. There is at the same time a double tangent joining points A and A', and a triple tangent between the three points B', B, and C. The latter line may be seen clearly in the enlarged view near $\varphi_1 = 1$ of Figure 3b, recalling that the tangent at B and C extends to B' as well. This case corresponds to intermediate values of α and T_{SN} . It is considered in order to see the tendencies in the phase diagram and the free energies when α increases and T_{SN} approaches T_{NI} . These

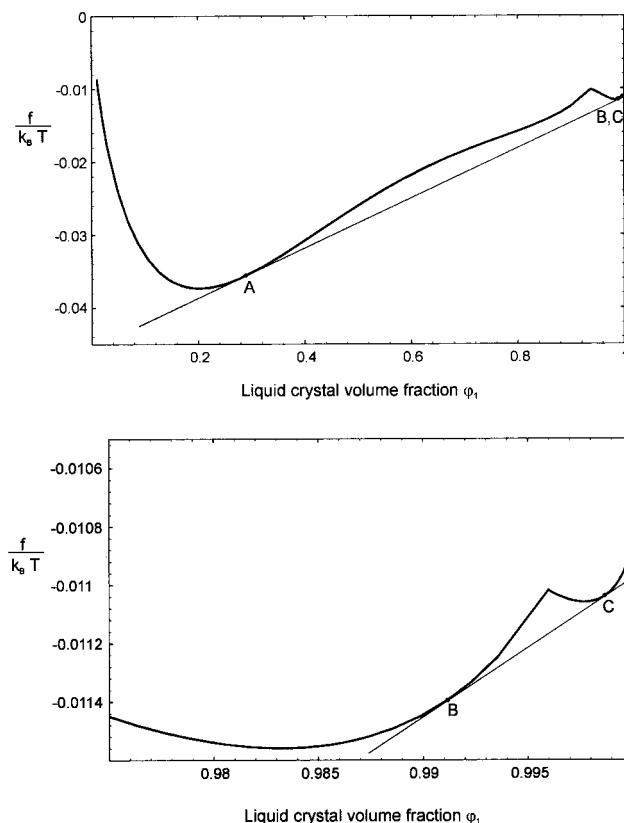


Figure 2. (a, top) Variation of the free energy density $f/(k_B T)$ as a function of φ_1 at $T = 39\text{ }^{\circ}\text{C}$ for a polymer/LC mixture characterized by $\alpha = 0.851$, $T_{SN} = 40\text{ }^{\circ}\text{C}$, and $T_{NI} = 60\text{ }^{\circ}\text{C}$. The free energy curve admits a triple tangent at this temperature. (b, bottom) Enlarged view of a in the vicinity of $\varphi_1 = 1$. The following parameters were used: $N_1 = 4$; $N_2 = 10$; and $\chi = -0.34 + 225/T$.

tendencies can be seen further by considering the third system with $T_{SN} = T_{NI} = 60\text{ }^{\circ}\text{C}$ and $\alpha = 0.98$. The free energy curve versus φ_1 of this mixture at $T = 51.2\text{ }^{\circ}\text{C}$ is shown in Figure 4. This figure is remarkably similar to the one corresponding to $T = 42\text{ }^{\circ}\text{C}$ for the nematic LC (Figure 2a in ref 12). The same triple tangent behavior is observed, but, nevertheless, substantial differences exist due to the fact that the single phase region near $\varphi_1 = 1$ corresponds to a smectic rather than a nematic phase. Below φ_{SI} , one has a region of two coexisting phases: one isotropic and one smectic. A direct transition takes place from smectic to isotropic phases.

(b) Phase Diagram. The critical interaction parameter for spinodal decomposition for an isotropic blend χ_C is given by the following expression within the Flory–Huggins lattice model¹³

$$\chi_C = \frac{1}{2} \left(\frac{1}{N_1^{1/2}} + \frac{1}{N_2^{1/2}} \right)^2 \quad (29)$$

Using this result and the relationship in eq 28 between χ and T yields the critical temperature $T_C = 61\text{ }^{\circ}\text{C}$. Likewise, within the same model, the critical volume fraction φ_C is given by

$$\varphi_C = \frac{N_2^{1/2}}{N_1^{1/2} + N_2^{1/2}} \quad (30)$$

which, according to the numbers $N_1 = 4$ and $N_2 = 10$,

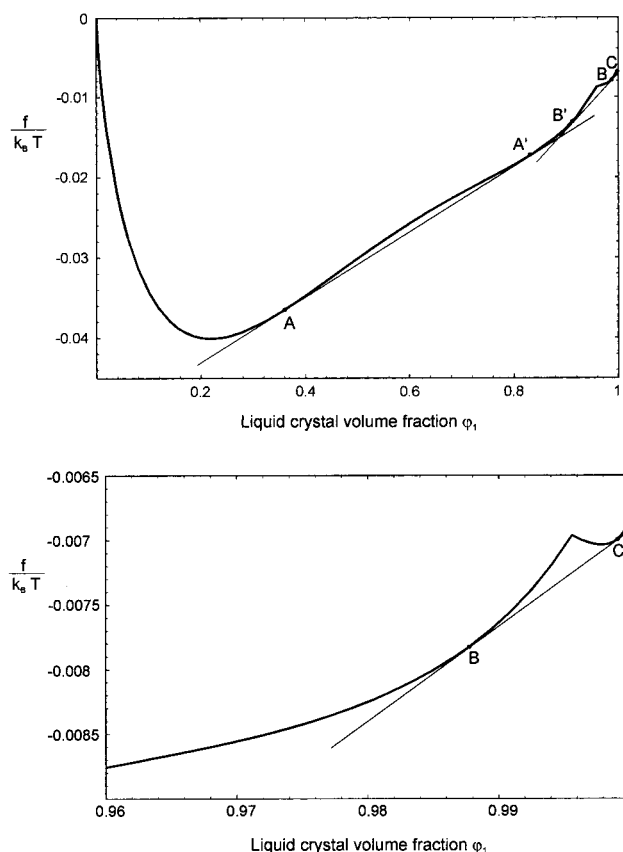


Figure 3. (a, top) Variation of the free energy density for a polymer/LC blend with φ_1 at $T = 46.3$ °C for $\alpha = 0.9$ and $T_{SN} = 48$ °C. The other parameters are the same as in Figure 2. (b, bottom) Enlarged view of a in the vicinity of $\varphi_1 = 1$.

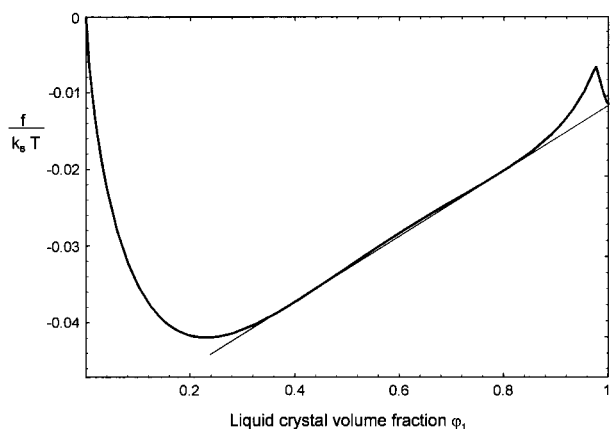


Figure 4. Free energy density curve versus φ_1 of a polymer/LC system with $\alpha = 0.98$ and $T_{SN} = T_{SI} = 60$ °C at $T = 51.2$ °C. The other parameters are the same as in Figures 2 and 3.

yields $\varphi_C = 0.6125$. Once the critical point is known, one can proceed to predict the complete phase diagram and construct binodal and spinodal curves, as we shall describe in the following sections.

(1) Binodals. Binodals are constructed by calculating the composition of the two coexisting phases α and β at each temperature. The following three phases are found in our diagrams: isotropic, nematic, and smectic-A phases. Binodals are obtained from the equality of chemical potentials of the two components in coexisting phases

$$\mu_1^{(\alpha)} = \mu_1^{(\beta)} \quad (31)$$

$$\mu_2^{(\alpha)} = \mu_2^{(\beta)} \quad (32)$$

The chemical potentials are obtained from the first derivatives of the free energy. They contain an isotropic and an anisotropic contribution

$$\mu_1 = \left(\frac{\partial F^{(i)}}{\partial n_1} \right)_{n_2} + \left(\frac{\partial F^{(a)}}{\partial n_1} \right)_{n_2} = \mu_1^{(i)} + \mu_1^{(a)} \quad (33)$$

$$\mu_2 = \left(\frac{\partial F^{(i)}}{\partial n_2} \right)_{n_1} + \left(\frac{\partial F^{(a)}}{\partial n_2} \right)_{n_1} = \mu_2^{(i)} + \mu_2^{(a)} \quad (34)$$

The explicit forms of isotropic and anisotropic chemical potentials are

$$\mu_1^{(i)} = \ln \varphi_1 + \left(1 - \frac{N_1}{N_2} \right) \varphi_2 + \chi N_1 \varphi_2^2 \quad (35)$$

$$\mu_2^{(i)} = \ln \varphi_2 + \left(1 - \frac{N_2}{N_1} \right) \varphi_1 + \chi N_2 \varphi_1^2 \quad (36)$$

$$\mu_1^{(a)} = -\ln Z + \frac{1}{2} (S^2 + \alpha \sigma^2) \nu \varphi_1^2 \quad (37)$$

$$\mu_2^{(a)} = \frac{1}{2} \frac{N_2}{N_1} (S^2 + \alpha \sigma^2) \nu \varphi_1^2 \quad (38)$$

Solving this set of equations yields the binodals. Figure 5a represents the results for $\alpha = 0.851$ and $T_{SN} = 40$ °C. It shows a diagram reminiscent of an upper critical solution temperature (UCST). It has regions of coexisting phases and regions of single phases. The diagram shows several biphasic regions: one isotropic–isotropic (I + I) region, two nematic–isotropic (N + I) regions, one smectic–nematic (S + N) region, and one smectic–isotropic (S + I) region. The anisotropic forces produce a region of a single smectic phase in the immediate vicinity of $\varphi_1 = 1$. This region is extremely narrow and can be visualized only if one considers an enlarged view near $\varphi_1 = 1$ as shown in Figure 5b. This figure shows clearly the single phase regions together with the regions of coexisting phases. The single nematic region near $\varphi_1 = 1$ is much wider and appears roughly at temperatures above T_{SN} . The fact that the nematic region is much wider than the smectic region indicates that more polymer molecules may be admitted into the less ordered nematic phase, while the highly ordered smectic phase has a stronger repulsion toward the polymer. Two eutectic lines are observed, the first one at $T = 39$ °C and hence below T_{SN} while the second is at $T = 42$ °C and hence above T_{SN} . The free energy curves at these two temperatures present triple tangents, but the phases in equilibrium of each case are different. At temperatures above T_{SN} , the diagram is similar to the one obtained for mixtures of linear polymers with nematic LCs.¹² However, two different (N + I) regions emerge. One of them is located between $T = 39$ °C and $T = 42$ °C and has an isotropic phase rich in polymer while the other region is located just above and has an isotropic phase rich in LCs. Figure 6a shows the diagram for another system characterized by $\alpha = 0.9$ and $T_{SN} = 48$ °C. Examples of free energy curves of this mixture are given in Figure 3a,b. This diagram shows also two eutectic lines at $T = 44$ °C and $T = 46.3$ °C, different biphasic regions such as (S + I),

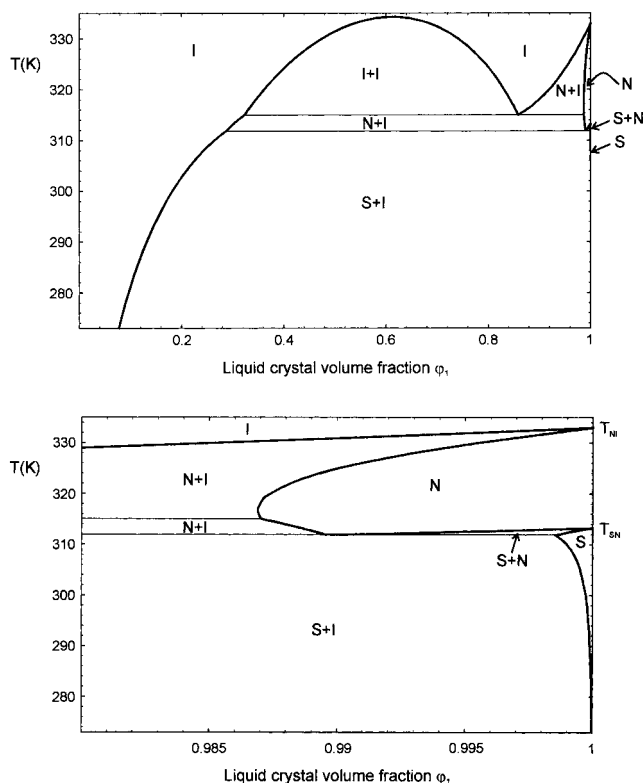


Figure 5. (a, top) Phase diagram of a linear polymer/smectic-A LC mixture using the same parameters as in Figure 2a,b. The single phase regions and the biphasic regions are indicated by capital letters: (I + I), isotropic–isotropic region; (N + I), nematic–isotropic region; (S + N), smectic–nematic region; (S + I), smectic–isotropic region. (b, bottom) Enlarged view of a near $\varphi_1 = 1$. The single nematic region above T_{SN} is much wider than the single smectic region.

(I + I), (S + N), and (N + I) and two regions with a single nematic N and a single smectic S phase. It reveals two (S + I) different regions: One of them has an isotropic phase rich in polymer and is located below the lower eutectic line. The other (S + I) region is much smaller and has an isotropic phase rich in LC located above the first eutectic line. Unlike Figure 5a, this figure shows only one biphasic region of (N + I) coexisting phases because the smectic ordering forces are stronger here. In the scale of this figure the single smectic phase region cannot be visualized clearly. An amplification of Figure 6a for the region near $\varphi_1 = 1$ is given in Figure 6b. Here, clearly visible are not only the single smectic and nematic phases but also the tiny region of (S + N) coexisting phases, which is not seen in Figure 5a. This region is also present in the preceding case for $\alpha = 0.851$ and $T_{SN} = 40^\circ\text{C}$, and its presence was first noted by Kyu and Chiu.²⁷ One difference between the two mixtures is that, in Figure 5, T_{SN} is located between the two eutectic lines, while, in Figure 6, T_{SN} is above the two lines. For temperatures exceeding T_{SN} , the phase behavior is similar to the case of nematic LC. Figure 7a shows the binodal of a polymer/LC blend for which the smectic parameter is $\alpha = 0.98$, and the transition temperatures T_{NI} and T_{SN} are equal ($T_{SI} = T_{NI} = 60^\circ\text{C}$). Beside the region of single isotropic and single smectic phases, one observes three biphasic regions of coexisting phases. One region of isotropic–isotropic (I + I) and two regions of smectic–isotropic (S + I) phases. The transition from smectic ordering to the isotropic phase occurs directly without the emergence of an intermediate nematic phase. More-

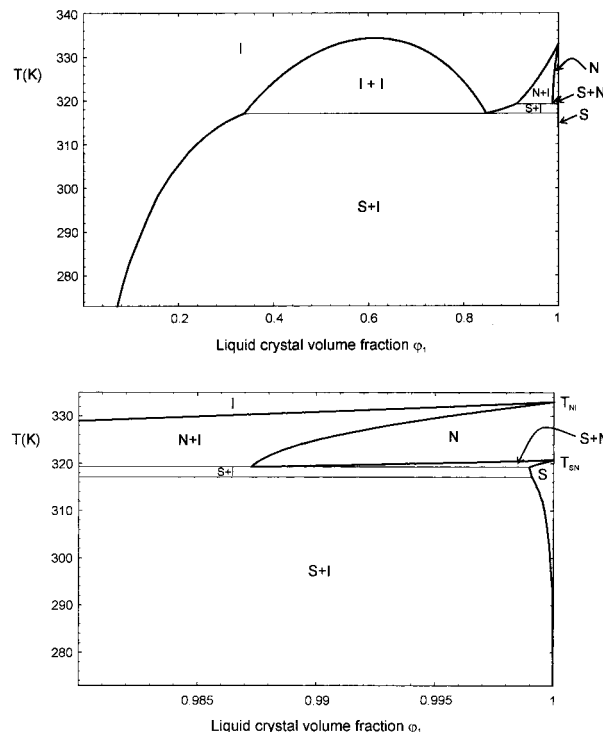


Figure 6. (a, top) Phase diagram of a linear polymer/smectic-A LC blend with $\alpha = 0.9$ and $T_{SN} = 48^\circ\text{C}$ in the same conditions as Figure 3a,b. There are several regions of coexisting phases (S + I), (I + I), (S + N), and (N + I) and two regions with a single nematic N and a single smectic S phase. There are two (S + I) different regions. (b, bottom) Enlarged view of a near $\varphi_1 = 1$. Unlike a, the single smectic, single nematic, and biphasic regions of coexisting (S + N) phases are clearly seen in this figure.

over, the region of single smectic phase is very close to $\varphi_1 = 1$ and can be distinguished only in the enlarged view of Figure 7b. In all parts of the diagram where a smectic phase appears, its LC volume fraction is very close to 1, implying that it is almost a pure LC phase. This is due to the fact that the well-ordered structure of smectic LC molecules is not compatible with the rather disordered polymer chains. This diagram looks quite similar to the diagram of nematic LC. The main difference is that, in the present case, one deals with higher ordered smectic phases. To see if there are other differences, we plot in Figure 8a the binodals for $\alpha = 0$ (nematic LC, thick line) and $\alpha = 0.98$ (smectic LC with $T_{SN} = T_{NI} = 60^\circ\text{C}$, dotted line), keeping the isotropic properties of the blend unchanged. Differences between the two cases are essentially due to the fact that the miscibility of smectic LC with the polymer is much more reduced than in the case of nematic LC. For the smectic LC system, the region of the single isotropic phase is smaller, the (I + I) region of isotropic coexisting phases shifts to higher temperatures, and the single smectic phase is also much narrower. The phase diagram near $\varphi_1 = 1$ is further illustrated in the enlarged view of Figure 8b. The single smectic phase shows a tiny strip near the axis $\varphi_1 = 1$. Since this phase is much narrower than the nematic phase, in turn the (S + I) region is much wider than the (N + I) region. If one considers a lower value of α and T_{SN} , the comparison with the case of nematic LC where $\alpha = 0$ reveals also differences which were not found in the present case. For example, Figure 9a shows the binodals for the systems characterized by $\alpha = 0.851$ ($T_{NI} = 60^\circ\text{C}$, $T_{SN} = 40^\circ\text{C}$, dotted line) and $\alpha = 0$ ($T_{NI} = 60^\circ\text{C}$, thick line). First, one notes

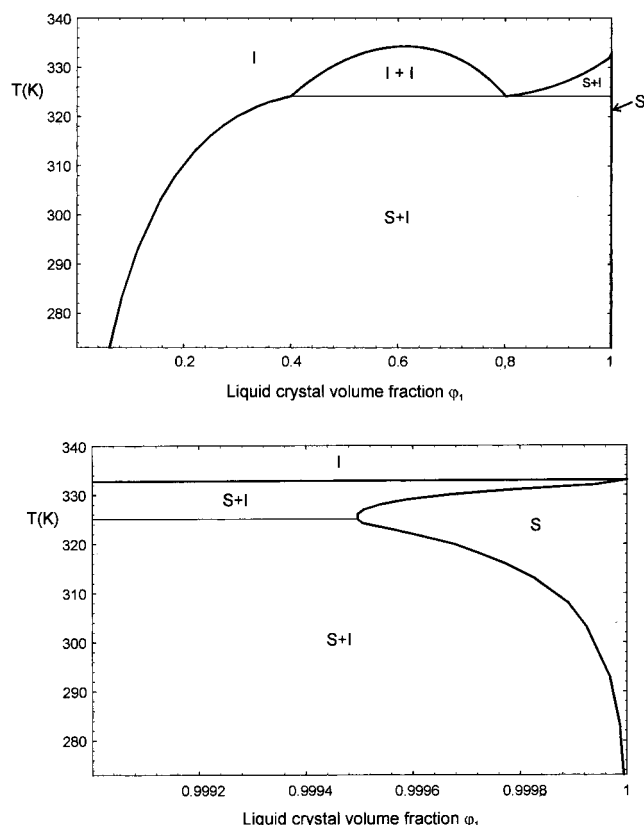


Figure 7. (a, top) Binodal of a linear polymer/smectic-A LC mixture with $T_{NI} = T_{SN} = 60$ °C and $\alpha = 0.98$. The other parameters are the same as in Figure 6a. Here, the transition from smectic to isotropic phases occurs directly without the intermediate nematic phase. (b, bottom) Enlarged view of a near $\varphi_1 = 1$, showing a sharp region of a single smectic phase.

that the binodal in the smectic LC is shifted to the left but less than in the case of Figure 8a. The (I + I) zone is also slightly reduced in favor of the (S + I) and (N + I) regions. The gap of miscibility is increased by the smectic ordering forces but to a lower extent than that in the previous case of Figure 8a. The (I + I) zone is also slightly reduced in favor of the regions (S + N) and (N + I). The gap of miscibility is increased by the smectic ordering forces. More details on the effects of smectic forces on the phase behavior are identified if one considers an enlarged view near $\varphi_1 = 1$, as one can see from Figure 9b. Unlike the case of Figure 8a,b ($\alpha = 0.98$), $T_{SN} = T_{NI}$ and one observes a biphasic region of (S + N) coexisting phases.

(2) Spinodals. To our knowledge, the spinodal curves for mixtures of polymers and smectic LCs have not been reported before. The equations of spinodals are obtained by letting the second derivative of the free energy with respect to φ_1 be zero. This means

$$\frac{\partial^2 f^{(i)}}{\partial \varphi_1^2} + \frac{\partial^2 f^{(a)}}{\partial \varphi_1^2} = 0 \quad (39)$$

The first term on the left-hand side of this equation gives the isotropic part of the spinodal equation within the Flory–Huggins lattice model and is given by

$$\frac{\partial^2 f^{(i)}}{\partial \varphi_1^2} = \frac{1}{N_1 \varphi_1} + \frac{1}{N_2 \varphi_2} - 2\chi \quad (40)$$

The anisotropic contribution to the spinodal equation

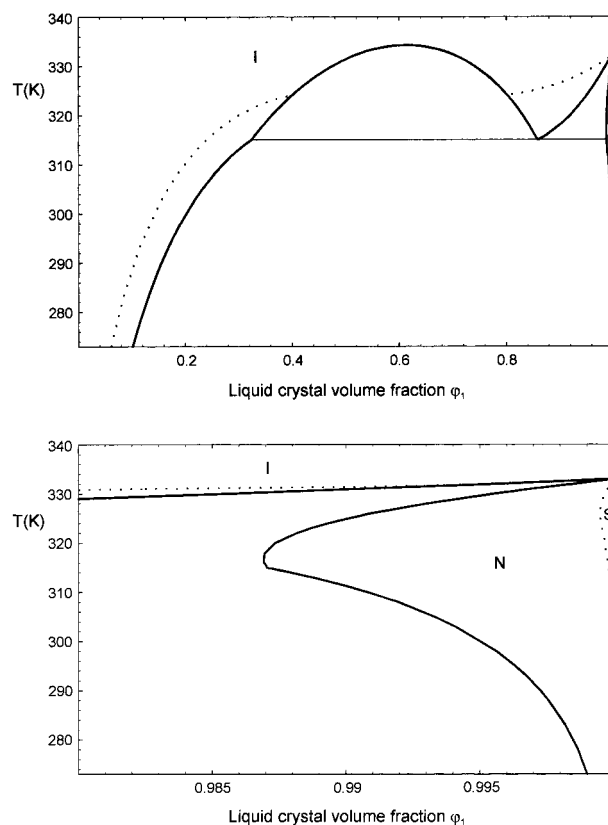


Figure 8. (a, top) Phase diagrams for linear polymer/LC mixtures for $\alpha = 0$ (nematic LC, thick line) and $\alpha = 0.98$ (smectic LC with $T_{SN} = T_{NI} = 60$ °C, dotted line). The other parameters are the same as in Figure 6a. The miscibility of the mixture is reduced remarkably when the order of LC is higher. (b, bottom) Enlarged view of a near $\varphi_1 = 1$. The single smectic phase is much narrower than the single nematic region.

is obtained from the Maier–Saupe–McMillan theory as follows:

$$\frac{\partial^2 f^{(a)}}{\partial \varphi_1^2} = -\frac{1}{N_1} \frac{\partial \ln Z}{\partial \varphi_1} \quad (41)$$

Combining this result with the expression for the anisotropic partition function Z yields

$$\frac{\partial^2 f^{(a)}}{\partial \varphi_1^2} = -\frac{\nu s}{N_1} \left(s + \varphi_1 \frac{\partial s}{\partial \varphi_1} \right) - \frac{\nu \alpha \sigma}{N_1} \left(\sigma + \varphi_1 \frac{\partial \sigma}{\partial \varphi_1} \right) \quad (42)$$

Substituting eqs 40 and 42 into eq 39 yields the spinodal equation, which can admit two or more solutions depending on the values of α , T , and φ_1 . Figure 10 shows the complete phase diagram for $\alpha = 0.851$ ($T_{SN} = 40$ °C), including both the spinodal (dashed curve) and the binodal (thick curve). The latter is taken from Figure 3 and is reproduced here for this system in order to complete the phase diagram. The first dotted line from the left represents the variation of φ_{NI} versus T , while the second represents φ_{SN} versus T . These two lines define the limits for the three spinodal branches. Unlike the case of nematic LC, there are three spinodal branches in this figure. The isotropic–isotropic (I + I) spinodal transition branch has the usual parabolic form and runs roughly from $\varphi_1 = 0.3$ ($T = 0$ °C) to the point where it intersects the dotted line for φ_{NI} after passing through the critical point at the peak. This branch is

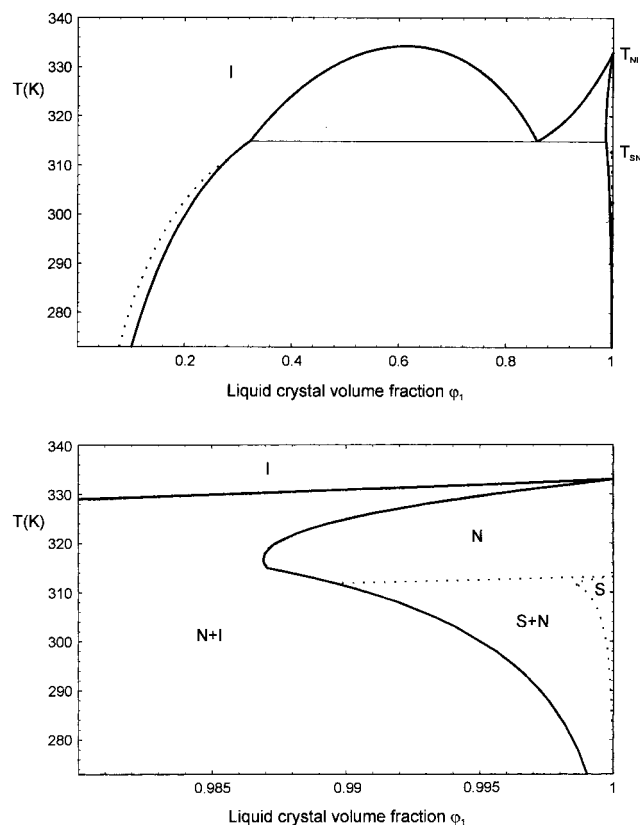


Figure 9. (a, top) Phase diagrams for linear polymer/LC mixtures with $\alpha = 0.851$ (smectic LC with $T_{NI} = 60^\circ\text{C}$, $T_{SN} = 40^\circ\text{C}$, dotted line) and $\alpha = 0$ (nematic LC with $T_{NI} = 60^\circ\text{C}$, thick line). The other parameters are the same as in Figure 6a. (b, bottom) Enlarged view of a near $\phi_1 = 1$. There is an additional region for $\alpha = 0.851$ with (S + N) coexisting phases.

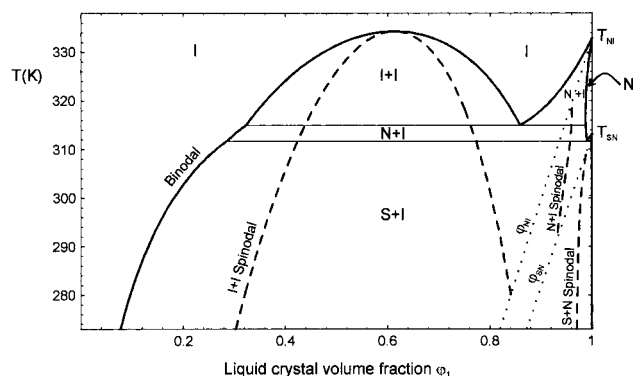


Figure 10. Complete phase diagram for a linear polymer/smectic-A LC mixture including the spinodal curve for $\alpha = 0.851$ ($T_{SN} = 40^\circ\text{C}$) represented by dashed lines. The thick line is the binodal curve of Figure 3. The first dotted line from the left represents the variation of ϕ_{NI} versus T , and the second corresponds to ϕ_{SN} versus T . The isotropic-isotropic (I + I) spinodal transition branch runs roughly from $\phi_1 = 0.3$ ($T = 0^\circ\text{C}$) to the point where it intersects the ϕ_{NI} dotted line. It is independent of the value of α . The nematic-isotropic (N + I) spinodal transition branch starts at the ϕ_{NI} line and ends at the ϕ_{SN} line. The smectic-nematic (S + N) spinodal transition branch starts upward at the ϕ_{SN} line.

independent of the value of α . The second branch describes the nematic-isotropic (N + I) spinodal transition. It has approximately a linear form and starts at the ϕ_{NI} dotted line and ends at the ϕ_{SN} line. The third branch corresponds to the smectic-nematic spinodal transition. It is similar to the latter branch and starts upward at the ϕ_{SN} line. Figure 11 shows the phase

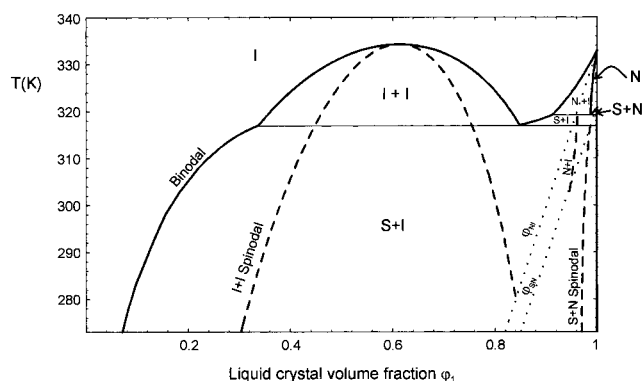


Figure 11. Same as Figure 10 with $\alpha = 0.9$ and $T_{SN} = 48^\circ\text{C}$.

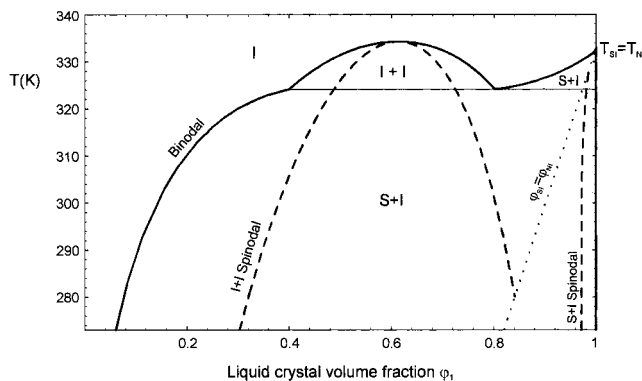


Figure 12. Same as Figure 10 with $\alpha = 0.98$ and $T_{SN} = T_{SI} = 60^\circ\text{C}$. The two dotted lines are superimposed. Only one smectic-isotropic spinodal branch subsists in addition to the (I + I) branch, which is the same as in the previous diagrams.

diagram for the polymer/LC mixture characterized by $\alpha = 0.9$ and $T_{SN} = 48^\circ\text{C}$. The difference with Figure 10 in terms of spinodal branches is essentially quantitative. The same qualitative observations apply here as well. But if one considers the third mixture with $\alpha = 0.98$ and $T_{SN} = 60^\circ\text{C}$, the situation is quite different since now $T_{NI} = T_{SN} = 60^\circ\text{C}$, $\phi_{NI} = \phi_{SN}$, and the two dotted lines are superimposed. The phase behavior of this mixture is illustrated in Figure 12, where only one smectic-isotropic spinodal branch subsists besides the (I + I) branch, which is the same as in the other cases.

For $\phi < \phi_{NI} = \phi_{SN}$ no smectic nor nematic orderings can take place, and the spinodal equation admits in general two solutions at each temperature except in two cases where the spinodal equation has only one solution: at the peak or critical point and below the point where the (I + I) branch intersects the ϕ_{NI} line.

3.3. Phase Diagrams for Blends of Smectic-A LCs and Cross-Linked Polymers.

The phase properties of mixtures of cross-linked polymers and nematic LCs were considered before.¹² If the polymer matrix consists of cross-linked polymer chains, the Flory-Huggins lattice model is not appropriate and the free energy should be modified to account for the elasticity of the network. The new form of the free energy induces important distortions in the phase diagram although the anisotropic free energy remains the same. To understand the effects of cross-links, a systematic study of thermodynamic properties of nematic LCs with both linear and cross-linked polymers was performed.¹² Here this study is extended to the case of smectic-A LCs in order to identify the combined effects of cross-links in the polymer matrix and smectic ordering in the LCs. Figure 13 represents the phase diagram for a mixture

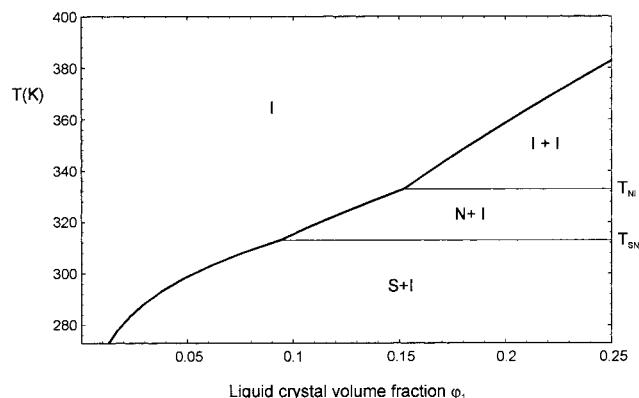


Figure 13. Phase diagram for a cross-linked polymer/smectic-A LC mixture with $N_c = 10$, $\alpha = 0.851$, and $T_{SN} = 40$ °C. The other parameters N_i , $\chi(T)$, and T_{NI} are the same as in Figure 6a.

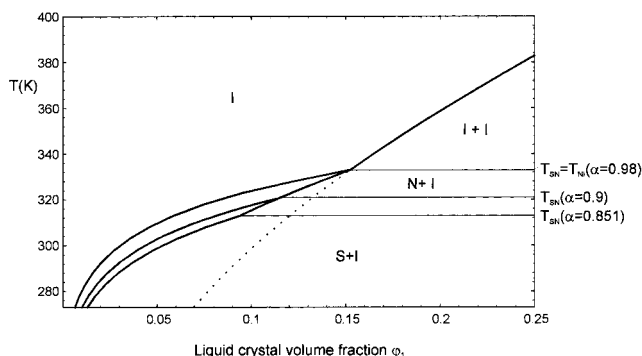


Figure 14. Same as in Figure 13 with three values of α . The extension above T_{NI} is the isotropic part, and its extension below T_{NI} is represented by a dotted line. The thick curves below T_{NI} are the binodals for $\alpha = 0.98, 0.9$, and 0.851 from left to right, respectively.

of a cross-linked polymer and a smectic-A LC with $\alpha = 0.851$, $T_{SN} = 40$ °C, and $N_c = 10$. The average number of monomer units between consecutive cross-links N_c is given arbitrarily the same value as the degree of polymerization N_2 only for the purpose of comparison between linear and cross-linked polymers. The nature of the phases are indicated on Figure 13. For the present value of α , there are three regions of coexisting phases. Below T_{SN} , there is an isotropic phase coexisting with a pure smectic-LC phase. In the region of temperature between T_{SN} and T_{NI} , the smectic order melts into a nematic order and one observes an isotropic phase coexisting with a pure nematic LC phase. Above T_{NI} , but below the binodal curve, one has two isotropic coexisting phases and the system behaves as a network-solvent mixture. An isotropic phase consisting of a network swollen by the LC coexists with a pure LC phase with randomly oriented molecules.

The phase behavior depends slightly on the value of α and T_{SN} . To understand such dependence, we show in Figure 14 the phase diagram for three mixtures characterized by different values of α . All of the other parameters are kept the same. The part of the curve common to the three mixtures above T_{NI} represents their extension of the isotropic binodal. The extension below T_{NI} of the isotropic branch is represented by a dotted line. The thick curves below T_{NI} are the binodals for $\alpha = 0.98, 0.9$, and 0.851 from left to right, respectively. This representation enables one to see how the phase diagram is distorted when the LC molecules are submitted to smectic forces with different strengths. As

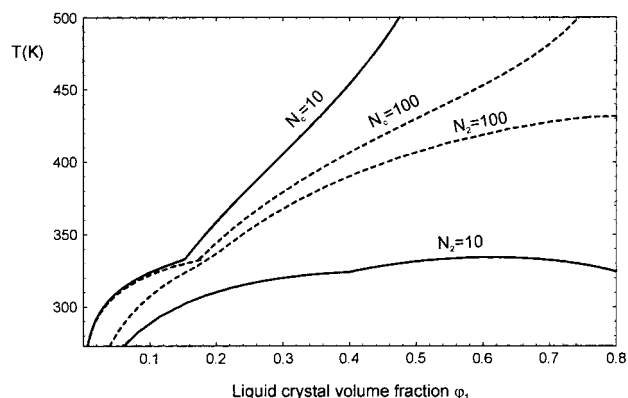


Figure 15. Binodals of cross-linked polymer/smectic-A LC mixtures and for linear polymer/smectic-A LC blends for $\alpha = 0.98$ and two values of $N_2 = N_c$. The thick lines correspond to $N_2 = N_c = 10$, and the dashed lines represent the results for $N_2 = N_c = 100$. The two upper curves correspond to the cross-linked polymer, whereas the two lower ones are binodals of the linear polymer.

the strength of these forces increases, the isotropic domain on the left of the binodals shrinks due to a loss of miscibility resulting from anisotropic forces. The region of N + I coexisting phases diminishes as α increases and disappears when α reaches the value 0.98, where $T_{NI} = T_{SI} = T_{SN}$. Above this temperature, the smectic order melts down into an isotropic phase directly.

To compare the phase diagrams of mixtures with linear and cross-linked polymers with different sizes, we let $\alpha = 0.98$ considering two values of $N_2 = N_c$. The results are shown in Figure 15, where the thick lines correspond to $N_2 = N_c = 10$ and the dashed lines to $N_2 = N_c = 100$. The upper two curves are established for the cross-linked polymer, whereas the lower ones are binodals for the linear polymer matrix. As N_2 and N_c increase, the binodals tend to approach each other with a more pronounced trend in the lower range of ϕ_1 and T . The effects of increasing N_2 and N_c on the phase diagram seem to evolve in opposite directions, whether one considers cross-linked or linear polymers. As N_2 increases, the miscibility of the linear polymer and LC decreases, whereas when the network mesh size N_c increases, it can admit more LC molecules in its volume and therefore show enhancement of compatibility. In general, however, anisotropic forces inducing nematic or smectic ordering do not favor mixing with disordered polymers. This behavior is valid for all the values of α considered.

4. Conclusions

The phase properties of polymer/LC mixtures with smectic-A LCs are investigated. Three systems are considered, corresponding to different values of the parameter α , which represents the strength of the smectic ordering forces. These parameters correspond to different temperatures of the smectic-nematic transition. The lowest value $\alpha = 0.851$ for which $T_{SN} = 40$ °C is 20 °C below the nematic-isotropic transition temperature T_{NI} . The phase diagram of this mixture shows noticeable differences compared with the case of nematic LC. These differences emerge through the appearance of a region of a single smectic phase and a biphasic region of smectic-nematic coexisting phases. Another system with $\alpha = 0.9$ and $T_{SN} = 48$ °C is considered and leads to similar observations with the

same quantitative discrepancies only. In both cases when one increases the temperature starting below T_{SN} , a sequence of different phases appears, starting from a smectic phase which first becomes a nematic phase for $T_{\text{SN}} < T < T_{\text{NI}}$ before melting down into an isotropic phase for $T > T_{\text{NI}}$. As α reaches the value 0.98, T_{SN} becomes equal to T_{NI} and one observes a direct transition from smectic to isotropic ordering, unlike the previous cases.

Blends of polymer and smectic-A LC are also studied in the case of cross-linked polymer chains. The effects of cross-links on the phase diagram are discussed. Substantial differences are found compared to linear polymers. One essential difference is the emergence of a pure smectic phase in a much narrower region near $\varphi_{\text{NI}} = 1$ than the pure nematic phase. Regardless of the polymer architecture, ordering forces do not favor mixing; the higher smectic ordering generates demixing interactions. Increasing the size of the linear polymer favors demixing, whereas an increase of the mesh size of the network N_c enhances its compatibility with the LC. As N_c increases, the difference between the phase properties of mixtures of LCs with linear or cross-linked polymers is reduced, especially in the lower range of φ_1 .

In this work, full phase diagrams are given, and for the first time, spinodal curves are shown for cross-linked polymers mixed with smectic-A LCs. In the case where T_{SN} is different from T_{NI} ($\alpha < 0.98$), the spinodal curve is made of three branches representing the isotropic–isotropic, nematic–isotropic, and smectic–nematic transitions.

The present formalism relies heavily upon mean field approximations at different levels. It has the merit of being simple and captures the essential qualitative features of the phase properties of mixtures made of polymers and smectic-A liquid crystals. Nevertheless it suffers from various shortcomings due essentially to the neglect of fluctuations which may become significant if one operates these systems in the immediate vicinity of the critical temperatures. In these regions, fluctuations become important and bear significant consequences, not only upon the thermodynamic behavior but also upon the quality of electrooptical response functions. The failure of mean field theories to describe properly the phase behavior of multicomponent critical mixtures has been discussed in various places, and it is beyond the scope of the present work to review these studies and their conclusions. The reader is referred to textbooks and specialized articles which discuss these subjects in more detail.^{11,28–30} We only make a few remarks in an attempt to put in a better perspective the aim of the present work and roughly show the limits of the validity of its findings.

Numerous experimental studies relying in particular on light scattering techniques illustrate the extent to which predictions of the mean field theories deviate from the observed data. In general, the qualitative features are captured quite well with the mean field views, but if one scrutinizes more closely the scattering data in the critical region, one observes substantial quantitative discrepancies of various types which are all due essentially to the effects of fluctuations.

The transition temperature itself may undergo a substantial shift³⁰ which renders the analysis of the critical behavior even more difficult since the range of temperature over which fluctuations should be included is hard to evaluate. In this respect, the concepts of

mean field critical temperature and Ising critical temperature or mean field and Ising critical exponents have been invoked sometimes to analyze the scaling behavior of strongly interacting polymer blends.

It is worthwhile recalling that the effects of fluctuations on various physical properties such as the forward scattering, the correlation length for critical fluctuations, the specific heat, the order parameters, and other relevant quantities are analyzed by examining the asymptotic behavior since these properties diverge in a well-defined manner when the critical temperature is approached and the regime of critical fluctuations sets in. Such divergences are governed by critical exponents which are sometimes quite distinct from the mean field predictions. Therefore, a quantitative investigation of the phase behavior in the critical region requires a more refined treatment which goes beyond the mean field view adopted here or even high order perturbation treatments. A possible way of implementing this generalization is to perform renormalization group calculations, where renormalized quantities are introduced. This method relies on a heavy mathematical formulation and permits depiction of the leading asymptotic behavior of the relevant physical properties.

In the problem of interest here, the effects of fluctuations arise at various levels. First, in the isotropic region, the interaction between the two constituents of the blend is controlled by the Flory–Huggins interaction parameter χ . At the temperature T_c , this parameter reaches a critical value χ_c which drives the mixture to phase separate into two isotropic phases of different compositions. In the case of polymers made of linear chains, the phase transition is described using the Flory–Huggins lattice model, which clearly needs to be improved if one seeks a genuine quantitative treatment near T_c . For our purpose in the present work, we think that such refinements are not necessary and do not lead to substantial improvements of the qualitative picture of the phase diagram. Similar observations can be made in the case of cross-linked networks, where the elasticity term of the matrix polymer due to cross-links is modeled following the Flory–Rehner model.^{13,20} Fluctuations affect quantitatively the properties governing swelling and deswelling of the network near T_c . Volume changes are described using a single parameter χ , which is assumed to be a function of the temperature only. This model is oversimplified, and its generalization to include the composition dependence of χ is currently under investigation.

In the conditions where anisotropic interactions are strong, ordered structures of different types take place. Below the nematic–isotropic transition temperature, the system exhibits a nematic long-range orientational order with angular fluctuations around a director. The properties of nematic liquid crystals are known to be extremely sensitive to external perturbations which give them a number of potential applications especially in display technologies. The presence of fluctuations may result in a change in the response of these systems to external perturbations via electric or magnetic field excitations, which is an important aspect to be kept in mind if one considers their potential applications in electrooptical devices. Below the nematic–smectic-A transition temperature, a smectic order appears with layered structures of well-defined interlayer spacings. The smectic liquid crystals are characterized by enhanced inertia as compared to nematic liquid crystals,

and, hence, they are more difficult to perturb. Their advantage, however, resides in their characteristic short time responses. In this case, fluctuations are capable of inducing shifts in the transition temperature smearing out the space density modulations.

In summary, our primary goal in this investigation is to predict the essential qualitative trends of the phase behavior of smectic-A liquid crystals and polymers with and without cross-links. All the refinements due to fluctuations near the transition temperatures are ignored. One of the main points is to show how the elasticity of the polymer network affects the phase diagrams of such composite materials.

Acknowledgment. This work has been accomplished within the scientific agreement CNRS/DRS. We thank these organizations for their kind support.

References and Notes

- (1) Chandrasekhar, S. *Liquid Crystals*, 2nd ed.; Cambridge University Press: Cambridge, U.K., 1992.
- (2) de Gennes, P. G. *The Physics of Liquid Crystals*; Oxford University Press: Ely House, London, 1974.
- (3) Doane, J. W. Polymer Dispersed Liquid Crystal Displays. In *Liquid Crystals: Their Applications and Uses*; Bahadur, B.; Ed.; World Scientific: Singapore, 1990.
- (4) Drzaic, P. S. *Liquid Crystal Dispersions*; World Scientific: Singapore, 1995.
- (5) Maschke, U.; Coqueret, X.; Loucheux, C. *J. Appl. Polym. Sci.* **1995**, *56*, 1547.
- (6) Maschke, U.; Coqueret, X.; Benmouna, M. *Polym. Networks Blends* **1997**, *7*, 23.
- (7) Maschke, U.; Traisnel, A.; Turgis, J.-D.; Coqueret, X. *Mol. Cryst. Liq. Cryst.* **1997**, *299*, 371.
- (8) Maschke, U.; Gogibus, N.; Traisnel, A.; Coqueret, X. *Liq. Cryst.* **1997**, *23*, 457.
- (9) Olabisi, O. L.; Robeson, L. M.; Shaw, M. T. *Polymer-Polymer Miscibility*; Academic Press: New York, 1979.
- (10) Kamide, K. *Thermodynamics of Polymer Solutions*; Elsevier Press: Tokyo, 1990.
- (11) de Gennes, P. G. *Scaling Concepts in Polymer Physics*; Cornell University Press: Ithaca, NY, 1979.
- (12) Benmouna F.; Bedjaoui L.; Maschke U.; Coqueret X.; Benmouna M. *Macromol. Theory Simul.*, in press.
- (13) Flory, P. J. *Principles of Polymer Chemistry*; Cornell University Press: Ithaca, NY, 1965.
- (14) Maier, W.; Saupe A. *Z. Naturforsch.* **1959**, *14A*, 882.
- (15) Maier, W.; Saupe A. *Z. Naturforsch.* **1960**, *15A*, 287.
- (16) (a) Shen, C. Ph.D. Dissertation, University of Akron, OH, 1995. (b) Shen, C.; Kyu, T. *J. Chem. Phys.*, **1995**, *102*, 556.
- (17) McMillan, W. L. *Phys. Rev. A* **1971**, *4*, 1238.
- (18) Bauer, B. J.; Briber, R.; Han, C. C. *Macromolecules* **1989**, *22*, 940.
- (19) Briber, R.; Bauer, B. J. *Macromolecules* **1991**, *24*, 1899.
- (20) Bastide, J.; Leibler, L.; Prost, J. *Macromolecules* **1990**, *23*, 1821.
- (21) James, H.; Guth, E. J. *J. Chem. Phys.* **1947**, *15*, 669.
- (22) Hermans, J. J. *J. Polym. Sci.* **1962**, *59*, 197.
- (23) Kuhn, W. J. *J. Polym. Sci.* **1946**, *1*, 183.
- (24) Flory, P. J. *J. Chem. Phys.* **1950**, *18*, 108.
- (25) Merck Liquid Crystals, Licrilite Brochure; Merck Ltd, Merck House: Poole, U.K., 1994.
- (26) Abramowitz, M.; Stegun, I. A. In *Handbook of Mathematical Functions*; Dover Publications Inc.: New York, 1972; p 376.
- (27) Kyu, T.; Chiu, H. W. *Phys. Rev. E* **1996**, *53*, 3618.
- (28) de Gennes, P. G.; Prost J. *The Physics of Liquid Crystals*; Oxford Science Publications, Clarendon Press: Oxford, U.K., 1995.
- (29) Morkvin, D. N.; Romanov, V. P. *Phys. Rev. E* **1994**, *49*, 4121.
- (30) Meier, G.; Momper, B.; Fischer, E. W. *J. Chem. Phys.* **1992**, *97*, 5884.

MA9804038